THE ASTROPHYSICAL JOURNAL, 392:678–690, 1992 June 20

SUPERHUMP TIMING IN SU URSAE MAJORIS SYSTEMS: IMPLICATIONS OF THE DATA FOR THE PRECESSING DISK MODEL

LAWRENCE A. MOLNAR AND HENRY A. KOBULNICKY[1]
Department of Physics and Astronomy, University of Iowa, Iowa City, IA 52242
Received 1991 August 14; accepted 1991 December 30

ABSTRACT

We tabulate the most current data for the orbital period, superhump period, and mass ratio in SU Ursae Majoris type variables to test models of the superhump timing mechanism. Contrary to earlier reports, the correlation between the superhump period excess and the orbital period is not significant. However, the correlation between the superhump period excess and the mass ratio is significant at the 4.7 σ level. This correlation was predicted by the Whitehurst model which explains superhumps as periodic enhancements of tidal dissipation in an eccentric, precessing accretion disk.

We compare these data with the results of recent hydrodynamical simulations and with our own calculations of coplanar, restricted three-body orbits as a function of mass ratio for mass ratios less than unity. We find that all reliable mass ratios for SU UMa systems are consistent with the upper limit of 0.22 placed by the model. We also computed the degree of instability as a function of mass ratio. We attribute the delays in the onset of superhumps observed in WZ Sge and WX Cet to the relatively small instability expected for their mass ratios. The theoretical superhump period computed by Whitehurst for a mass ratio of 0.15 agrees well with the data, but the values computed by Hirose & Osaki are systematically too high. Stringent further tests of the model are afforded theoretically by trying to reproduce the observed superhump period–mass ratio relationship, and from observation by further exploring the time delay–mass ratio relationship. If the validity of the model can be established in this way, superhump timing observations can serve as a much-needed tool for determining mass ratios in SU UMa systems.

Finally, we review the status of proposed models for the superoutburst cycle in SU UMa systems.

Subject headings: binaries: close — instabilities — novae, cataclysmic variables

1. INTRODUCTION

SU Ursae Majoris type variables are a class of nonmagnetic dwarf novae with orbital periods among the shortest of any cataclysmic variables. Warner (1985) reviewed the observational properties of SU UMa systems. Of the 19 systems with measured orbital periods, 18 have periods of less than 2 hours, the lower edge of the period gap. SU UMa systems undergo outbursts which fall into two categories: (1) *normal* outbursts, which last from 2 to 4 days and are characterized by an increase in total system brightness of about 3 mag, and (2) less frequent but quasi-periodic *super*outbursts, which typically last 10–14 days and are roughly a magnitude brighter than the normal outbursts. Observationally, superoutbursts appear to evolve from normal outbursts (van der Woerd & van Paradijs 1987). An additional modulation of the light curve of up to 0.5 mag, called the "superhump," is observed only during superoutburst, and has become the defining characteristic of SU UMa systems. The superhump is seen in systems of all inclinations, implying a physical event in the system rather than a geometric effect. Superhumps do not appear until after the rise to maximum light, and then they recur with periods that range from 0.8% to 9% longer than the orbital period. While the superhump period in a given system is similar from one superoutburst to the next, four systems have exhibited a slowly decreasing period over the course of a superoutburst. WZ Sge and similar systems show longer superoutbursts and fewer normal outbursts than other SU UMa systems, but are better characterized as at the extreme of a continuum rather than as a qualitatively different class of dwarf novae.

Numerous models have been proposed to account for superhumps (Papaloizou & Pringle 1979; Vogt 1982; Whitehurst, Bath, & Charles 1984; Warner 1985; Osaki 1985; and Whitehurst 1988). However, most models make no specific predictions about superhump timing, nor do they explain the period distribution of SU UMa systems. The model of Papaloizou & Pringle (1979) offered the first quantitative prediction of superhump timing, but their relation produced a maximum superhump period that is only 1.5% longer than the orbital period, in sharp disagreement with the observations. Whitehurst (1988) presented hydrodynamic simulations in which superhumps were produced by periodic enhancements of tidal dissipation in an eccentric, precessing accretion disk, and which reproduced the superhump period of the well-observed system Z Cha. In this paper we critically examine the Whitehurst (1988) superhump model as presented in that paper and as further developed by Osaki (1989), Hirose & Osaki (1990), and Whitehurst & King (1991). We also comment on the implications for models of the superoutburst cycle.

In § 2 we tabulate for all known SU UMa systems the best published measurements of the quantities most relevant to the model: orbital period, superhump period, and mass ratio. We also tabulate available data on candidate SU UMa systems. In § 3 we compare these data with the results of the hydrodynamical simulations of Whitehurst (1988) and Hirose & Osaki (1990). We also present the results of coplanar, restricted three-body orbital stability calculations which illuminate some of the processes underlying the hydrodynamical simulations. In § 4 we review the Osaki (1989) and Whitehurst & King (1991)

[1] Present address: Department of Astronomy, University of Minnesota, 116 Church Street, S.E., Minneapolis, MN 55455.

models for superoutburst cycles, emphasizing their differing motivations and predictions. Finally, in § 5 we summarize our conclusions and highlight the further theoretical and observational work needed to test the eccentric disk model rigorously. An appendix contains a detailed discussion of our three-body calculations in relation to previous work.

2. THE DATA

In Tables 1 and 2 we compile the best published measurements (and uncertainties) of the three parameters necessary to describe superhump timing in the Whitehurst model: the orbital period, P_o; the superhump period, P_s; and the mass ratio, $q \equiv m_2/m_1$, where m_1 is the mass of the white dwarf primary and m_2 is the mass of the Roche lobe–filling companion. The final column of each table lists the literature references for the three quantities, with dashes where no reference applies. For those systems which exhibit a range of superhump periods, we list the maximum and minimum observed periods.

In Table 1 we include systems for which the orbital period and superhump period have both been measured. Where published sources have inexplicably not included uncertainties, we have estimated them, footnoting each instance. Where published mass ratios based on conservative assumptions exist, we have listed them. Where there are no reliable estimates of mass ratios, we have generally estimated them by assuming the companion to be a main-sequence star described by Patterson's (1984) equation (7) relating orbital period to companion mass, and by assuming the white dwarf mass to be in the wide, illustrative range of 0.4–1.0 $M_\odot$. In the following we discuss the exceptional but important cases of WZ Sge and T Leo.

For WZ Sge, Gilliland, Kemper, & Suntzeff (1986) have estimated a mass ratio of 0.09, based on measurements of the K_1 velocity in quiescence. However, as the phase of the S-wave with respect to the eclipse is *not* that expected for the white dwarf, both their assumption that the measured K_1 velocity is that of the white dwarf and the mass ratio derived from this

TABLE 1

SU URSAE MAJORIS SYSTEMS WITH DETERMINED ORBITAL AND SUPERHUMP PERIODS

Name	$P_o(\sigma_o)$ (days)	$P_s(\sigma_s)$ (days)	$q\ (=m_2/m_1)$	References
WZ Sge	0.0566878455(7)	0.05714(94)	<0.23[a]	1, 2, 3
SW UMa	0.056810(69)	0.05833(6)	0.153(0.043)	4, 5, 6
T Leo	0.058819(5)	0.06414(4)[b]	0.51(0.04)	7, 8, 7
VY Aqr	0.060(1)[c]	0.06445(1)[c]	0.20(0.09)[d]	9, 10, –
V436 Cen	0.0625(2)	0.06383(2)	$0.167(^{+0.022}_{-0.062})$	11, 12, 11
OY Car	0.0631209239(5)	0.064245(46)	0.102(0.003)	13, 14, 13
TY Psc	0.0639(42)	0.07014(61)[e]	0.21(0.09)[d]	14, 15, –
IR Gem	0.0684(6)	0.0708(4)	0.22(0.09)[d]	16, 17, –
AW Gem	0.073(6)	0.07867(1)[c]	0.25(0.11)[d]	18, 6, –
HT Cas	0.0736472070(24)	0.076077(74)	0.15(0.03)	19, 19, 20
VW Hyi	0.07427111(6)	0.07712–0.07623[f]	0.171(0.027)	21, 22, 23
Z Cha	0.074499215(66)	0.07725(2)	0.150(0.003)	24, 25, 26
WX Hyi	0.0748134(2)	0.0774(1)	0.196(0.054)	23, 23, 23
SU UMa	0.076351(43)	0.07882(7)	0.26(0.11)[d]	27, 28, –
BR Lup	0.08216(70)[c]	0.0822(2)	0.28(0.12)[d]	29, 30, –
TY PsA	0.08400(6)	0.08765(1)[c]	0.28(0.12)[d]	31, 31, –
YZ Cnc	0.0868(2)	0.0920–0.0905[f]	0.30(0.13)[d,g]	32, 33, –
TU Men	0.1176(18)	0.12625–0.12469[f]	0.35(0.10)[h]	34, 34, 34

[a] See text.

[b] Using the times of superhump maxima from Kato & Fujino 1991, we perform a least-squares fit with equal weighting to obtain this superhump period and uncertainty. Our period is consistent with theirs.

[c] Authors do not provide error estimates. We assume an uncertainty of 1 in the last decimal place, or 1 minute in cases where the superhump period is given only to the nearest minute.

[d] There are no reliable data on the mass ratios in these systems. To find plausible ranges, we adopt Patterson's 1984 eq. (7) relating the orbital period to the mass of the (main-sequence) secondary, and we take 0.4–1.0 $M_\odot$ as a wide, illustrative range for the mass of the white dwarf in calculating the mass ratio.

[e] Author quotes private communication giving P_s at 101 minutes. We assume an uncertainty of 1 minute.

[f] Designates observed ranges in the superhump period over the course of an outburst.

[g] The upper limit to q is based on a lower limit to the white dwarf mass of 0.75 $M_\odot$ from the HWZI of the Balmer absorption lines (Shafter & Hessman 1987).

[h] The upper limit to q is based on a lower limit to the white dwarf mass of 0.54 $M_\odot$ from the HWZI of the Balmer absorption lines (Stolz & Schoembs 1984).

REFERENCES.—(1) Robinson et al. 1978; (2) Patterson et al. 1981; (3) Gilliland et al. 1986; (4) Shafter et al. 1986; (5) Robinson et al. 1987; (6) Ritter 1990; (7) Shafter & Szkody 1984; (8) Kato & Fujino 1991; (9) Augusteijn & Della Valle 1990; (10) Grauer & Bond, private communication cited in Warner & Livio 1987; (11) Gilliland 1982a; (12) Semeniuk 1980; (13) Wood et al. 1989; (14) Schoembs 1986; (15) Szkody & Feinswog 1988; (16) Feinswog et al. 1988; (17) Szkody et al. 1984; (18) Howell & Szkody 1988; (19) Zhang et al. 1986; (20) Horne et al. 1991; (21) Vogt 1974; (22) Vogt 1983; (23) Schoembs & Vogt 1981; (24) Cook & Warner 1984; (25) Vogt 1982; (26) Wood et al. 1986; (27) Thorstensen et al. 1986; (28) Udalski 1989; (20) O'Donoghue, reported in Warner & Livio 1987; (30) O'Donoghue 1987; (31) Warner et al. 1989; (32) Shafter & Hessman 1987; (33) Patterson 1979; (34) Stolz & Schoembs 1984.

assumption are suspect. Because WZ Sge has the shortest orbital period of all the systems, its companion is also the least likely to be on the main sequence. We therefore set an upper limit on the mass ratio of 0.23 based on the following assumptions: (1) the main-sequence mass (0.10 $M_\odot$) is an upper limit to the companion mass and (2) the HWZI of the Balmer emission lines (Gilliland et al. 1986) represents the velocity of the inner disk and may be no greater than the Keplerian velocity at the star's surface, thus placing a lower limit on the mass of the white dwarf (0.44 $M_\odot$).

For T Leo, Shafter & Szkody (1984) give upper limits to the masses of the companion and white dwarf of 0.19 and 0.4 $M_\odot$, respectively. However, their assumptions may be used to estimate a mass ratio as well. Shafter & Szkody require the orbital inclination, i, to be less than $\sim 65°$ based on the lack of eclipses and orbital humps. Based on the observed HWZI of 1900 km s^{-1}, they further set a limit on the mass of the white dwarf:

$$m_1 > \frac{0.29}{(\sin i)^2} M_\odot , \quad (1)$$

requiring the mass of the white dwarf to be greater than 0.35 $M_\odot$ for an inclination of 65°. Their K_1 velocity of 135 ± 8 km s^{-1} and the mass function,

$$\frac{m_2^3 (\sin i)^3}{(m_2 + m_1)^2} = \frac{K_1^3 P_o}{2\pi G} , \quad (2)$$

place a further constraint. With the final constraint that m_2 be no greater than the main-sequence value (which Shafter & Szkody quote as 0.17 $M_\odot$, slightly higher than that obtained with the Patterson 1984 relation), the only self-consistent parameter set is with (m_1, m_2, i) equal to (0.35 $M_\odot$, 0.17 $M_\odot$, 65°). The resulting mass ratio is 0.51 ± 0.04, with the uncertainty dominated by the uncertainty on K_1.

T Leo is also unusual in having the greatest difference between the superhump and orbital periods, with a fractional superhump period excess, $\Delta P/P_o \equiv (P_s - P_o)/P_o$, of 0.090. We have rederived the superhump period from the data of Kato & Fujino (1991). While we find a second minimum at a period excess of 0.027, the rms residual of this fit (11 minutes) is twice that of the published figure. We therefore conclude this to be an alias, and support the published figure as the superhump period.

In Table 2 we list systems in which superhumps have been observed but measurement of the orbital period is lacking, and we list systems whose outburst behavior makes them SU UMa candidates, although no superhumps have yet been observed. We do not estimate uncertainties or mass ratios if they are not provided in the original sources. We also include EX Hya in our list, although it is thought to be an intermediate polar (DQ Her), the only one below the period gap. The Whitehurst (1988) model suggests that the superhump behavior resides in the outer disk of systems with extreme mass ratios. As the outer disk is thought to be intact in intermediate polars, this lone system with an extreme mass ratio is a good candidate for

TABLE 2

INCOMPLETELY OBSERVED SU URSAE MAJORIS SYSTEMS AND SU URSAE MAJORIS CANDIDATES

Name	$P_o(\sigma_o)$ (days)	$P_s(\sigma_s)$ (days)	$q(=m_2/m_1)$	References
WX Cet	NA[a]	0.05304(3)	NA	–, 1, –
CY UMa	NA	0.0593(NA)	NA	–, 2, –
EK TrA	NA	0.06492(10)	NA	–, 3, –
UV Per	NA	0.0663(3)	NA	–, 4, –
AQ Eri	NA	0.06703(NA)	NA	–, 2, –
SS UMi	NA	0.070(NA)	NA	–, 5, –
RZ Sge	NA	0.07035–0.07000[b]	NA	–, 6, –
FO And	NA	0.073(NA)	NA	–, 7, –
AY Lyr	NA	0.075970(18)	NA	–, 8, –
CU Vel	NA	0.0799(NA)	NA	–, 9, –
EX Hya	0.0682338367(10)	NA	0.12[c]	10, –, 10
TT Boo[d]	NA	NA	NA	–, –, –
UZ Boo[e]	NA	NA	NA	–, –, –
AL Com[e]	NA	NA	NA	–, –, –
V503 Cyg[d]	NA	NA	NA	–, –, –
V1504 Cyg[d]	NA	NA	NA	–, –, –
AH Eri[d]	NA	NA	NA	–, –, –
V592 Her[e]	NA	NA	NA	–, –, –
RZ Leo[d,e]	NA	NA	NA	–, –, –
CY Lyr[d]	NA	NA	NA	–, –, –

[a] The orbital of WX Cet is subject to contention. Van Paradijs et al. 1989 say the orbital period is uncertain, but likely near 6.98 hr. Szkody et al. 1989 list a value of 127 ± 5 minutes. O'Donoghue et al. 1991 note that these value are inconsistent with their observed superhump period near 80 minutes.

[b] Designates observed ranges in the superhump period over the course of an outburst.

[c] Figure quoted by authors as a plausible value, subject to large uncertainty.

[d] Cited by Kuulkers 1990 as possible SU UMa candidates based on their outburst behavior.

[e] Cited by Richter 1992 as possible SU UMa candidates based only on their outburst recurrence time.

REFERENCES.—(1) O'Donoghue et al. 1991; (2) Ritter 1990; (3) Vogt & Semeniuk 1980; (4) Udalski & Mattei 1989; (5) Chen et al. 1991; (6) Bond et al. 1982; (7) Grauer & Bond 1986, reported in Szkody et al. 1989; (8) Udalski & Szymanski 1988; (9) Vogt 1982; (10) Gilliland 1982b.

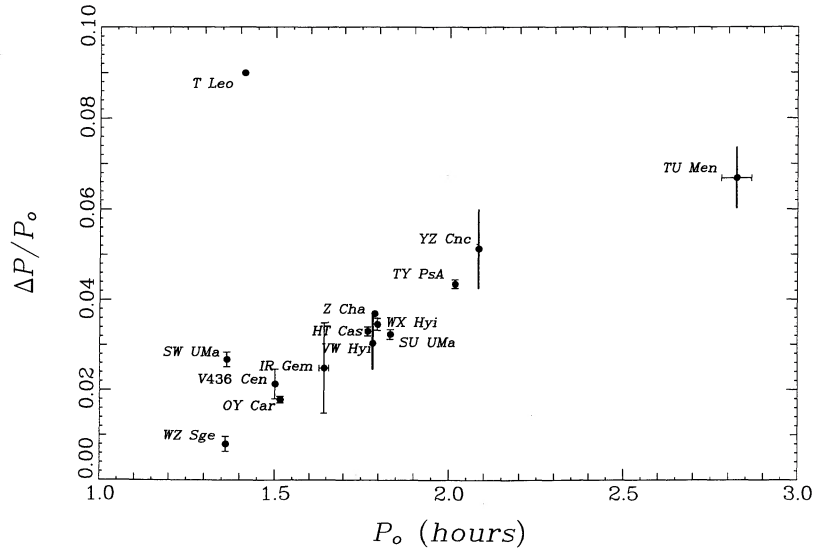

FIG. 1.—Superhump period excess vs. orbital period in hours for the 14 SU UMa systems in Table 1. Uncertainties are not plotted where they are smaller than the symbols. Where ranges in the superhump period have been observed, we denote the ranges with vertical lines rather than with error bars with serifs.

superhumps should there be a superoutburst. Data which complete Table 2 will be helpful in further evaluating models of superhumps and superoutbursts.

Stolz & Schoembs (1984) and Robinson et al. (1987) showed evidence for a correlation between the orbital period and the superhump period. In Figure 1 we plot $\Delta P/P_o$ versus P_o for all systems in Table 1 for which the period excess is determined to better than $\sim 1\%$, a total of 14 systems. We distinguish the systems with observed ranges in the superhump period from the others by using lines rather than error bars with serifs. The correlation of these two parameters for these systems is *not* significant, since the correlation coefficient is 0.43, corresponding to a significance of 1.5 σ. The low correlation coefficient is largely due to T Leo, although the period excess of SW UMa is significantly greater than that of WZ Sge despite the similar orbital periods. The period excess of VY Aqr (which was not included in the calculation) is also significantly greater than the excesses of other systems with similar orbital periods.

In Figure 2 we plot $\Delta P/P_o$ versus q for the same 14 systems. Systems for which the mass ratio estimate is based on assumptions of a main-sequence secondary are plotted with filled circles. Filled squares are used to denote systems for which no assumptions about the nature of the companion are made. As described in the next section, Whitehurst & King (1991) predict that this figure should show a monotonic relationship between the parameters. Omitting for the moment WZ Sge, for which

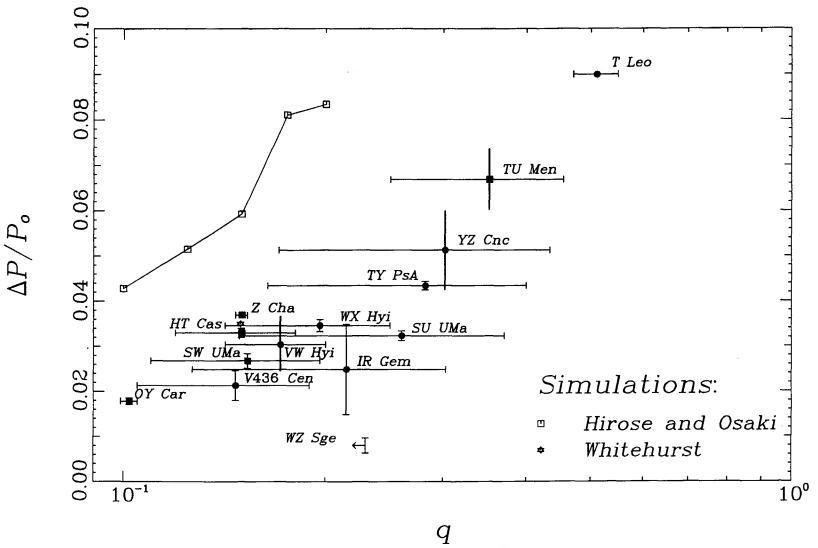

FIG. 2.—Superhump period excess vs. mass ratio for the 14 SU UMa systems in Table 1. Filled circles represent the observed values where the mass ratio is based on the assumption of a main-sequence companion. Filled squares are used when this assumption is not made. Where ranges in the superhump period have been observed, we denote the extent of the variations with horizontal lines rather than with error bars with serifs. The open star marks the period excess from the hydrodynamic simulations of Whitehurst (1988). Open squares mark period excesses from the hydrodynamic simulations of Hirose & Osaki (1990).

there is only an upper limit on mass ratio, we find a correlation between the parameters significant at the 4.7 σ level (correlation coefficient of 0.94).

Since orbital period is generally expected to correlate with mass ratio, it is no surprise to see the good correlation between period excess and mass ratio, given previous reports of the correlation between period excess and orbital period. Indeed, the period excess–orbital period relation remains good as a general rule, having but three exceptions: T Leo, SW UMa, and VY Aqr. But because our purpose is to determine which is the fundamental relationship and which the corollary, the identification of exceptions is central. Correlation analysis clearly favors models based on mass ratio (such as the Whitehurst model) over those based on orbital period.

The Whitehurst model predicts that beyond a simple correlation the relationship should be strictly monotonic. Given the typically large uncertainties on mass ratio, it is more difficult for the data to make a strong statement here, but, since a single well-established exception could challenge the model, we evaluate the model consistency on this point. We find that all of the data are consistent with $\Delta P/P_o$ being a strictly monotonic function of q to within the uncertainties. In order to determine the significance of the strict monotonicity, we shuffled the 14 values of q among the 14 $\Delta P/P_o$ values 100,000 times, noting the number of reorderings that were inconsistent with a monotonic relationship. We found 184 shufflings in 100,000 produced such a monotonic relation, making this distribution inconsistent with a random distribution at the 3.0 σ level. In Figure 3 we plot a histogram of the number of data pairs inconsistent with monotonicity in each shuffling. To test the robustness of this result, we performed the same procedure leaving individual points out of the data one at a time. Removing OY Car from the data has the largest effect, resulting in 720 reorderings that were consistent with monotonic. The distribution is then inconsistent with random at the 2.8 σ level.

With its large uncertainty in mass, VY Aqr is also consistent with a strict monotonic relationship. Such a relationship would require the white dwarf mass in VY Aqr to be relatively low, while that in TU Men must be relatively high. This consequence is amenable to an observational check (up to an ambiguity about inclination) by observation of the HWZI of the Balmer lines of VY Aqr.

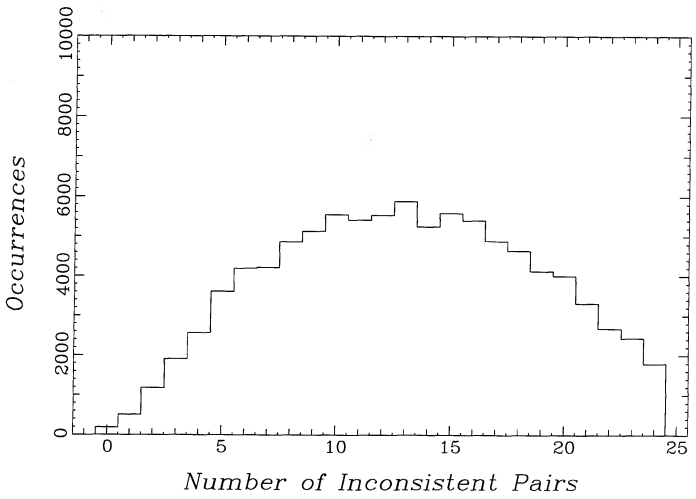

FIG. 3.—Histogram of the number of data pairs inconsistent with monotonicity in each of 100,000 reorderings of the data from Fig. 2.

3. DISCUSSION OF THE WHITEHURST MODEL

3.1. *Formation of an Eccentric Accretion Disk*

The essential feature of the Whitehurst (1988) superhump model is an eccentric accretion disk around the white dwarf which precesses slowly in the inertial reference frame of the binary system. The superhump period is identified with the synodic or beat period between the orbital period of the binary and the precession period of the disk. Variations in tidal stresses on the eccentric disk over the course of the orbit modulate the viscous dissipation of energy with the superhump period.

Whitehurst (1988) suggests that an eccentric disk will form naturally as the result of a regime of unstable orbits in systems with sufficiently extreme mass ratios. The presence of the eccentric disk is determined by the relative sizes of the "tidal truncation radius" and the "stability radius." For a disk with low pressure and viscosity around an isolated star, the gas should be in a family of concentric, circular Keplerian orbits. One can define the extension of this family to a binary as a set of concentric periodic orbits in the corotating frame. Piotrowski & Ziolkowski (1970) defined the stability radius as the radius of the smallest of these orbits which, when subject to a small radial perturbation, deviates ever further from the original orbit. Define the corotating coordinate system so that the two stars lie on the x-axis with the origin at the center of mass. Consider the stability of an orbit that intersects the x-axis at a point x_0 away from the primary with a velocity at that point in the y-direction with amplitude $\dot{y}_0$. Perturb the particle from this position a distance Δx_0, simultaneously changing the velocity so as to conserve the Jacobi integral,

$$C = \frac{1}{2}(x^2 + y^2 - \dot{x}^2 - \dot{y}^2) + \frac{1}{(q+1)d_1} + \frac{q}{(q+1)d_2}, \quad (3)$$

where d_1 is the distance between the particle and the white dwarf and d_2 is the distance between the particle and the companion. The Jacobi integral is the sole conserved quantity in the restricted three-body problem. The stability parameter, identified with the Lyapunov exponent, is then

$$a = \frac{\Delta x_1}{\Delta x_0}, \quad (4)$$

where Δx_1 refers to the offset from the reference position after one orbit. A value of $|a| > 1$ indicates an unstable orbit. Paczyński (1977) noted that one also reaches a "last nonintersecting orbit," beyond which orbits in this family intersect each other. The low-viscosity assumption must break down at this point, so that the last nonintersecting orbit is likely a close approximation to the tidal truncation radius, the point at which the tidal influence of the companion truncates the viscous expansion of the disk. See the Appendix for more discussion of the physical interpretation of these critical radii.

Whitehurst (1988) found that a Keplerian disk would develop an eccentric outer edge due to tidal interactions when the tidal truncation radius of the disk exceeds the stability radius. Paczyński (1977) found this inequality to be satisfied for mass ratios less than 0.22. (This has been inaccurately quoted as 0.25 in each of the superhump model papers discussed here.)

In order to define more exactly the conditions under which this instability may affect the orbits of material in the accretion disk, we computed a series of coplanar, restricted three-body orbits, investigating the stability of periodic orbits as a func-

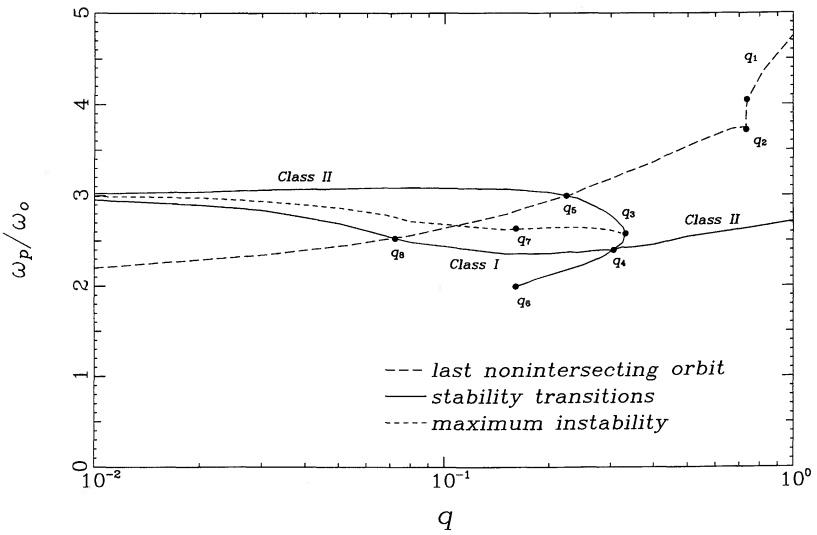

FIG. 4.—Particle frequency divided by orbital frequency vs. mass ratio for a number of critical orbits. The long-dashed line indicates the last nonintersecting orbit. The solid lines represent transitions in the stability parameter between stability and instability. The short-dashed line marks the local maxima of the instability parameter within the first unstable region. The critical points q_n are discussed in detail in the Appendix.

tion of mass ratio and the orbital frequency of the test particle, ω_p. This quantity, measured in the inertial frame of reference, is analogous to radius but better defined for the highly noncircular orbits in the outer disk. We summarize the results of these calculations in Figure 4, in which we plot the mass ratio of the system, q, against the normalized particle frequency ω_p/ω_o, where ω_o is the binary orbital frequency. Smaller values of ω_p/ω_o correspond to larger orbital radii.

The long-dashed line in Figure 4 indicates the frequency of the last nonintersecting orbit. The solid lines represent transitions in the stability parameter, a, between stability and instability. They delimit two unstable regions, one between the two lines that emanate from near $\omega_p/\omega_o = 3$ for low values of q, and the other in the lower right-hand portion of the figure. The short-dashed line marks the local maxima of the instability parameter, $|a|$, within the first unstable region. A detailed explanation of the lines and the critical points, q_n, is given in the Appendix.

The model of Whitehurst invokes the first unstable region. This unstable region first appears at a mass ratio of 0.33, denoted q_3, but is entirely beyond the last nonintersecting orbit at this point. As noted above, the maximum q that is both within the unstable region and interior to the last nonintersecting orbit is 0.22, denoted q_5. For $q < 0.08$ (q_8), the orbits become stable again before reaching the last nonintersecting orbit, as was first noted by Paczyński (1977) (cf. his Fig. 4). At more extreme mass ratios, the unstable region becomes increasingly narrow but *does not entirely disappear even out to mass ratios of* 10^{-7}! However, the maximum value of the instability parameter asymptotically approaches unity at small q, indicating that ultimately this range of orbits is marginally stable, and a real disk will be able to expand viscously beyond this region. This can be seen in Figure 5, in which we plot the maximum value of the instability parameter as a function of mass ratio. Figure 5 peaks at a mass ratio of 0.16 (point q_7 on Fig. 4), which therefore is the mass ratio for which the instability should be most effective. Note that the second unstable region can never be of interest to disks, since it lies entirely beyond the last nonintersecting orbit.

3.2. *The Range of Mass Ratios: Model and Data*

Based on the foregoing discussion, we expect the onset of instability in tidally truncated disks in systems with mass ratios up to 0.22. As the mass ratio decreases below 0.16, the instability becomes progressively weaker, so that we may expect its onset to be delayed, or not to occur at all for sufficiently low mass ratio systems. Whitehurst & King (1991) postulated that viscous forces could enable the disk to grow somewhat beyond the last nonintersecting orbit, making it possible to achieve instability at mass ratios beyond 0.22, out perhaps to the edge of the unstable region ($q_3 = 0.33$). The validity of this postulate is beyond the scope of a three-body calculation, since the intersection of the particle orbits implies that such a disk must be treated hydrodynamically. Hirose & Osaki (1990) performed hydrodynamic simulations for a range of mass ratios from 0.05 to 1.0 and found precessing disks only for mass ratios from 0.10 to 0.20, but not for 0.05 or 0.25 and above, consistent with the expectations based on the restricted three-body calculations.

The quoted lower limits of 12 of the 14 SU UMa systems in Figure 2 are consistent with an upper limit on the mass ratio of 0.22. Our nominal lower limit on TU Men is 0.25, assuming a main-sequence companion of 0.25 $M_\odot$ and a 1.0 $M_\odot$ white dwarf. However, a mass ratio less than 0.22 is very plausible if the companion is slightly undermassive (as is expected just above the period gap) or if the white dwarf is in the 1.1–1.3 $M_\odot$ range.

The lower limit on the mass ratio of T Leo described in § 2 is 0.47, based on measurements of K_1, the HWZI of Balmer emission, and an upper limit on the inclination. This is in serious disagreement with the model expectations. The mass ratio of T Leo can be reduced to 0.22 only by reducing K_1 by 6 σ to 87 km s^{-1}. (Allowing an inclination up to 90° reduces the change in K_1 to 5 σ. Reducing the mass ratio only to 0.33 reduces the change in K_1 to 3.4 σ.) Since we have already seen that the apparent K_1 velocity in WZ Sge does not reflect the motion of the white dwarf in that system, it seems more likely that the Whitehurst model can be used here to point out a problem in interpretation of the K_1 velocity of T Leo than that the T Leo mass ratio presents a problem for the Whitehurst model.

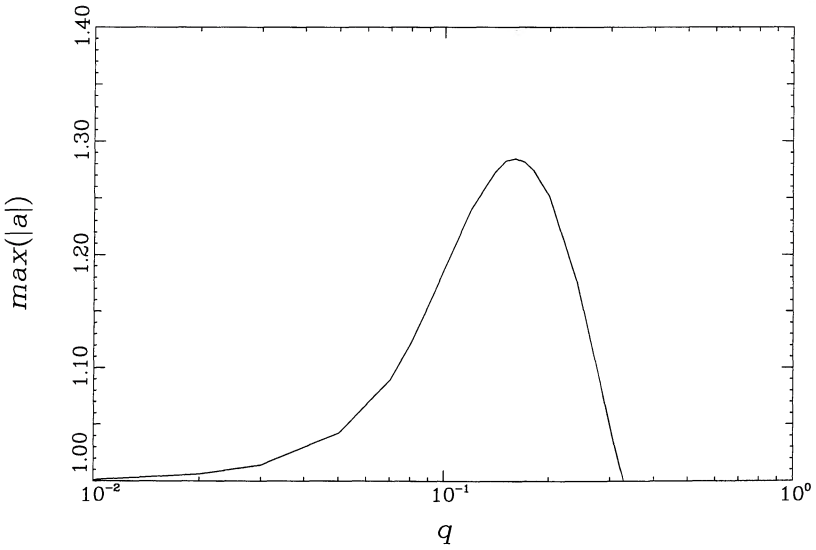

FIG. 5.—Maximum absolute value of the instability parameter vs. mass ratio

All 14 upper limits on mass ratio in Figure 2 are consistent with a lower limit of 0.1. As seen in Figure 5, the maximum value of the instability parameter at this mass ratio is still within 40% of its overall maximum, although it is rapidly dropping at this point toward lower mass ratios. While we have no firm value for the mass ratio of WZ Sge, the empirical result of a monotonic relationship between period excess and mass ratio implies that it has the smallest mass ratio of the systems in Figure 2. The superhumps of WZ Sge are distinctive in that it took a record 13 days from the commencement of the 1978 superoutburst for the superhumps to appear (Patterson et al. 1981). We suggest that this longer time scale is consistent with the model, since the much smaller degree of instability in this extreme mass ratio system would increase the time required to develop the disk eccentricity fully. In general, we expect the superhump start-up time to be directly correlated with mass ratio (and hence period excess) for the lower mass ratio systems. O'Donoghue et al. (1991) reported that WX Cet did not show superhumps until at least 4 days, and perhaps as many as 7 days, after the start of the superoutburst. While neither the mass ratio nor the orbital period of this system is known, its superhump period is the shortest known, suggestive of a low mass ratio system. The start-up time is between that of WZ Sge and OY Car (which showed superhumps by 3 days after maximum in 1985 May; Naylor et al. 1987). Hence we predict a period excess for WX Cet between 0.8% and 1.8%, or an orbital period between 75 and 76 minutes.

We conclude that all current data on SU UMa systems are consistent with the 0.22 $M_\odot$ upper limit on the mass ratio imposed by the Whitehurst model. There is no observational need to suppose that the tidal radius significantly exceeds the radius of the last nonintersecting orbit. We also find that the observation of longer superhump start-up times in very low mass ratio systems provides additional support for the model.

3.3. *Superhump Timing: Model and Data*

Hirose & Osaki (1990) show analytically that the transition to instability is due to a 3:1 parametric resonance between particle orbits and the companion star. Whitehurst & King (1991) show with restricted three-body calculations that a family of doubly periodic orbits exists (i.e., orbits in a 3:1 resonance), and that the first unstable orbit is a member of this family. (See the Appendix for a further description of this.) Whitehurst & King find further that, in their hydrodynamic simulations, an outer rim forms around the disk which has a doubly periodic orbit. The superhump period is identified as the time for material in the rim to complete its double loop. This is a special case of the general identification of the superhump period with the beat period between the orbital period of the binary and the precession period of the disk.

For the isolated particle in a resonant orbit the superhump period is easy to compute, being twice the particle period in the corotating frame:

$$\frac{P}{P_o} = \frac{2}{\omega_p/\omega_o - 1} . \tag{5}$$

The relevant values of ω_p are those of the top solid line in Figure 4, which range from 3 at 0.22, increase by several percent going toward lower q, and then asymptotically return to 3 for very large q. Hence, in the mass range of interest, the period excess for isolated particles in a doubly periodic orbit is *never* positive, contrary to all of the data. The analytic formula of Hirose & Osaki (1990) estimates precession rates as a function of particle radius and mass ratio in the more general, nonresonant Keplerian case. This formula yields only positive period excesses, with greater values at larger radii or larger mass ratios. We performed numerical simulations which confirm the general properties of their formula away from resonant orbits, although the actual values differ by as much as a factor of 2 in the region of interest. (This discrepancy is not surprising given the approximations of small radius and mass ratio intrinsic to the derivation.) Precession in a successful model, therefore, must be in either a nonresonant orbit, a non-Keplerian orbit, or both.

Whitehurst (1988) performed hydrodynamic simulations to obtain a superhump period excess of 3.5% for a mass ratio of 0.15. He used a short episode of mass transfer to initiate the development of an eccentric disk. Whitehurst & King (1991) note that the positive period excess found in the simulations is

due to the interaction of the rim with the disk, pushing it to a longer orbit. Hence their superhump model calls for resonant but non-Keplerian orbits. They claim that the magnitude of this effect is determined entirely by the mass ratio (not by the viscosity) and should increase with increasing mass ratio. Thus they predict a strictly monotonic relationship between period excess and mass ratio, although the detailed shape of this function awaits further computation. As the hydrodynamic effects must push the particle period several percent longer just to reach a superhump period excess of zero, it is possible that negative period excesses will result from simulations of very low mass ratio systems.

We plot the Whitehurst (1988) theoretical period excess with a star in Figure 2, where it is in good agreement with the SU UMa data. As discussed in § 2, the data are also entirely consistent with a strictly monotonic relationship, as Whitehurst & King (1991) require.

Hirose & Osaki (1990) determined period excesses from hydrodynamic simulations of mass ratios of 0.1, 0.125, 0.15, 0.175, and 0.2 using a constant mass transfer rate. We plot these results with open squares in Figure 2, and note that they fall systematically well above the SU UMa data and the Whitehurst (1988) model datum. Hirose & Osaki also differ from Whitehurst and King in their interpretation of the simulations. While they note the importance of the resonance for initiating the instability, their superhump model calls for particles in nonresonant orbits at slightly smaller radii. In this model, a decreasing radius through a superoutburst cloud naturally lead to a decreasing superhump period, as seen in some systems.

We conclude that the eccentric disk model provides a simple theoretical reason for the monotonic relationship between period excess and mass ratio, and has shown promise for reproducing the details of that relationship, although there are significant discrepancies between the results of different workers at present. In particular, the importance of the resonant orbit for the superhumps remains in dispute. In general, a strong test of the models will be to reproduce the details of the empirical period excess–mass ratio relationship with no free parameters, particularly the systems at the extremes: WZ Sge and T Leo. If this is done, the model can serve as a useful tool for determining reliable mass ratios from observations of period excess.

A second test of the models will be to reproduce the spatial distribution of light on the disk from superhumps revealed by eclipse mapping. While none of the models are advanced enough yet for detailed comparison, we note that the three enhanced regions found by O'Donoghue (1990) in his map of Z Cha correspond to the three points at which the doubly periodic orbit intersects itself (as seen, for example, in Fig. 3*a* of Whitehurst & King 1991), providing preliminary support for the importance of resonant orbits.

4. THE NATURE OF SUPEROUTBURSTS

While there is a consensus that normal outbursts are the result of thermal instabilities in the accretion disk, the nature of superoutbursts remains unclear, and even their precise definition is in dispute. Observations have established a number of characteristics that any superoutburst model must address: (1) superhumps occur only during superoutbursts; (2) superoutbursts evolve from outbursts (van der Woerd & van Paradijs 1987); (3) normal outbursts are unpredictable, but superoutbursts occur at more predictable intervals (Vogt 1980); (4) in VW Hyi the average energy emitted in normal outbursts in the time between superoutbursts is found to be correlated with the phase of the superoutburst cycle (van de Woerd & van Paradijs 1987).

The superoutburst property that is in dispute is their orbital period distribution. Some workers restrict the name "superoutburst" to only those systems which show superhumps, which, as we have seen, are the relatively short-period, extreme mass ratio systems. Others also include in the definition of superoutburst the wide outbursts of longer period systems such as SS Cyg, which shows a pattern of alternating wide and narrow outbursts (e.g., Hempelmann & Kurths 1990). There is as yet no observational distinction (beside the absence of superhumps) to exclude long-period systems. However, there is also no theoretical necessity to include these systems, since the alternating patterns may find an explanation in the details of the thermal instability model (e.g., Smak 1984).

Osaki (1989) suggested a model for superoutbursts which assumes that the rate of mass transfer from the companion is constant, and combines the effects of the thermal disk instability with those of the tidal instability. Thermal instabilities in the disk cause periodic episodes of accretion which are seen as normal outbursts, but the size of the disk is small enough that tidal torque is inefficient, so the enhanced viscosity of the outburst leads to expansion of the outer disk. The outer radius of the accretion disk expands farther with each successive outburst until the rim exceeds the tidal stability radius. With the next outburst, efficient tidal torque drives the eccentricity that produces superhumps and clears the outer disk. The heavy accretion from the outer disk enables the thermal instability to last longer and reduces the disk radius back to its starting point.

In this scenario, wide outbursts in long-period systems without superhumps would be accounted for by a separate mechanism, since the tidal instability that produces the superhumps also drives the superoutburst. The scenario naturally explains the evolution of a superoutburst from a normal outburst. The quasi-periodic nature of the superoutbursts is explained by the constant rate of mass transfer from the companion. The increasing normal outburst energy with supercycle phase may be explained as an increase in tidal torque with increasing disk radius. An important test of this model would be observational verification of the variation of disk radius with supercycle phase.

Whitehurst & King (1991) argue for the importance of the accretion stream in triggering the development of superhumps, noting that with no accretion stream the time scale for the instability is much longer than observed. They suggest, therefore, that the essence of the superoutburst is a period of enhanced mass transfer from the companion. A normal outburst presumably serves as the trigger for the enhanced mass transfer, accounting for the evolution of a superoutburst from a normal outburst. This model accounts naturally for superhumps occurring only during superoutburst. In this scenario wide outbursts in long-period systems may be accounted for by the same trigger as for the short-period systems. The lack of superhumps is merely an indication of the greater mass ratio. However, with no mechanism yet given for how the trigger operates, items 3 and 4 on our list remain unexplained, as does the alternating pattern seen in the wide systems. Whitehurst & King also cannot rule out the Osaki (1989) model yet, as they have not computed the time scale for the instability in the presence of a steady accretion stream.

5. CONCLUSIONS

Using data from 14 SU UMa systems, we show that the previously reported correlation between orbital period and superhump period excess is no longer significant. However, we show for the first time that the superhump period excess is significantly correlated with binary mass ratio and, furthermore, is consistent with a strictly monotonic relationship.

We compute coplanar, restricted three-body orbits to describe regions of stability for systems with mass ratios less than unity. In particular, we computed the degree of instability as a function of mass ratio of the unstable zone which Whitehurst (1988) suggested to be the source of disk eccentricity in SU UMa systems. We find that this zone extends to arbitrarily small mass ratios, but with an asymptotically vanishing degree of instability.

We find that the data support the Whitehurst (1988) model for superhumps in a number of ways. All reliable estimates of SU UMa mass ratios are consistent with the upper limit allowed by the model (0.22). Whitehurst & King (1991) argue that the period excess should be a unique, monotonic function of mass ratio, which we find to be true. There is evidence that systems with mass ratios below 0.1 show increasing time delays before the onset of superhumps, consistent with the decreased degree of instability in these systems. The model value for period excess for a mass ratio of 0.15 found in hydrodynamic simulations by Whitehurst (1988) agrees well with the data, although the values found by Hirose & Osaki (1990) are systematically high.

Further theoretical work should focus on determining a model period excess–mass ratio relationship, and on resolving the importance of the resonance to the observed superhump period. If more complete calculations are in consonance with the data presented here, this would be a powerful verification of the model. It would also be an extremely useful tool for the identification and further study of other puzzling properties of SU UMa systems. For example, the Whitehurst paradigm identifies the K_1 velocity of T Leo as anomalously high, adding it to the puzzle of the anomalous phase of the K_1 measurements in WZ Sge. Also, with some assumptions about the companion masses, the distribution of white dwarf mases in SU UMa systems could be determined. Also needed are theoretical investigations of the delay in the onset of superhumps and the decreasing superhump period observed in some systems.

In order to test the model further, detailed observations should focus on systems at the extremes of period excess: their mass ratios and superhump start-up times. To make use of the model, orbital and superhump periods should be sought for the systems listed in Table 2.

The question of the superoutburst mechanism itself remains open. Simulations of superhump onset times with varying mass transfer rates may determine whether the root is in a disk instability (as suggested by Osaki 1989) or in a mass transfer instability (as suggested by Whitehurst & King 1991). An observational test of the former model is measurement of disk radii throughout a superoutburst cycle. The latter model needs to be extended to have a mechanism for triggering the mass transfer instability. This mechanism can be tested by the varying recurrence properties of superoutbursts as a function of orbital period.

Note added in manuscript.—One may use the empirical period excess-mass ratio relationship presented here to evaluate whether anomalous periods in other systems may arise from the same disk resonance. Grindlay et al. (1988) found an optical modulation in the X-ray burst source 4U 1915−05 with an 0.84 hr period, 1% longer than the X-ray dipping period. Rappaport & Joss (1984) derived a companion mass between 0.008 and 0.1 $M_\odot$, which implies q in the range 0.006–0.07 assuming a 1.4 $M_\odot$ neutron star. It is not immediately clear how to apply the superhump model, since the optical period is more stable than the X-ray period, so superhumps are not being directly observed in the optical as in the case of SU UMa systems. Nonetheless, a period excess of +1% is consistent with $q = 0.07$, or a period excess of −1% may be consistent with a smaller q, so it is reasonable to try to develop a superhump model for this system.

By contrast, Tuohy et al. (1990) found a photometric period in the cataclysmic variable 1H 0709−360 that is either 2.1% longer or 2.8% shorter than the orbital period (the two possibilities being aliases of each other). A superhump model would be applicable for a mass ratio near 0.15 or much less than 0.1, respectively. But these values are inconsistent with the estimate of Bailey (1990) that $q > 0.6$ or the general expectation of a high value of q for a system in a 2.4 hr orbit, so a superhump model does not seem reasonable for this system.

We thank Joe Patterson, Yoji Osaki, and an anonymous referee for valuable comments. This research has made use of the Simbad data base, operated at CDS, Strasbourg, France, This paper is dedicated to the memory of our coleagues and friends Christoph Goertz, Dwight Nicholson, Linhua Shan, and Robert Smith, who died on 1991 November 1 at the University of Iowa.

APPENDIX

As described in § 3.1, in Figure 4 we plot normalized particle frequency versus mass ratio for several critical orbits, based on our own prograde, coplanar, restricted three-body orbit calculations (Copenhagen class g orbits; Szebehely 1967). The long-dashed line in Figure 4 indicates the frequency of the last nonintersecting orbit. The solid lines represent transitions in the stability parameter, a, between stability and instability. The short-dashed line marks the local maxima of the instability parameter, $|a|$, within the first unstable region. We mark eight critical points q_n on Figure 4 to which this discussion will refer. Although portions of these results have been described in previous publications (Piotrowski & Ziolkowski 1970; Paczyński 1977; Whitehurst & King 1991), we wish to present a more comprehensive description which builds upon those works, filling in some gaps.

In this Appendix we will describe in more detail the number and nature of these crossings as a function of mass ratio, plotting for several representative mass ratios the families of singly and doubly periodic orbits as a function of the Jacobi integral, C, and the points at which the orbits cross the x-axis with velocity perpendicular to the x-axis. Using the notation of Paczyński (1977), orbital

radii at the x-crossing opposite the companion are designated r_1, and the radii at the x-crossing between the two stars as r_2. Doubly periodic orbits that have velocity perpendicular to the x-axis on the r_1 side we label class I doubly periodic orbits, and likewise those on the r_2 side we label class II doubly periodic orbits.

As described in § 3.3, Whitehurst & King showed that the first unstable orbit is in fact the orbit at which a class of doubly periodic orbits crosses the family of singly periodic orbits. It turns out more generally that each transition in the stability parameter is marked by such a crossing. The upper solid line, extending from ω_p/ω_o just above 3 for small values of q out through the critical points q_5, q_3, q_4, to q_6, is determined by the intersection of class II orbit families with the singly periodic orbit family. The lower solid line, extending from ω_p/ω_o just below 3 for small values of q out through the critical points q_8 and q_4 to just below q_3, is determined by the intersection of class I orbit families with the singly periodic orbit family. From the point on the lower solid line just below q_3 over to q of unity, it is determined by the intersection of a class II orbit family with the singly periodic orbit family. Hence there are between one and three doubly periodic orbit families, depending on the mass ratio. Those discussed in Whitehurst & King (1991) are only the one family at each mass ratio with the highest frequency.

Our Figure 4 is a more precise version of Figure 1 of Whitehurst & King (1991). They use their figure (which has analytic approximations of the 2:1 resonance, the 3:1 resonance, and the last nonintersecting orbit) to argue in general terms for the relevance of the 3:1 resonance to disk instability. (Note that they use the labels 3:1 and 3:2 interchangeably.) A comparison of the figures indicates some limitation of their argument. Since they represent the 3:1 resonance as a single line, rather than the two lines in our figure, the separation into two regions of instability described in § 3.1 (and indeed in the text of Whitehurst & King) cannot be represented. The intersection of the 3:1 resonance and the last nonintersecting orbit lines (q_5 on Fig. 4) is well represented in their Figure 1, although the value of q_5 is given as 0.33 rather than 0.22. The intersection of the 2:1 resonance and the last nonintersecting orbit lines in their Figure 1 implies that a new unstable region begins at that point ($q = 0.025$). However, we find no such region. Just as the 3:1 resonance is related to doubly periodic orbits in the corotating frame, the 2:1 resonance is related to singly periodic orbits in the corotating frame. The last nonintersecting singly periodic orbit *is* itself the manifestation of the 2:1 resonance. Note that the last nonintersecting orbit goes to an orbital frequency of 2 in the limit of small q.

We organize our detailed description of the behavior of the single and doubly periodic orbits by describing the situation at a mass ratio of unity fully and then noting for descending mass ratio what changes take place at each critical point.

A1. $q = 1.0$

In Figure 6*a* we plot, for a mass ratio of unity, C as a function of the r_1 crossing for two families of singly periodic orbits. The lines are solid for stable orbits and dashed for unstable orbits. Figure 6*b* is a similar plot of the r_2 crossings. Particle orbits in accretion disks would evolve down the branch with the higher value of C. This is the Copenhagen first phase, while the other family is the Copenhagen third phase (Szebehely 1967). Note that the first-phase orbits are double-valued in Figure 6*b*. The point of inflection here, which we mark with a filled circle in both Figures 6*a* and 6*b*, is the last nonintersecting orbit.

Also appearing in Figure 6*b* is a class II family of doubly periodic orbits, marked with a short-dashed line. The point at which this family of orbits intersects the singly periodic family is marked with a filled square in both Figures 6*a* and 6*b*. As discussed above, this is also a transition from unstable to stable orbits. There are two other transitions from unstable to stable, which occur at extrema in the value of C. Note, however, that all of the orbits out to the last nonintersecting orbit are stable.

A2. $q_1 = 0.734$

At q_1 the phase 1 and phase 3 orbits connect at the points of C extrema, and thereafter there is a phase consisting of the stable portions of phases 1 and 3, and another phase consisting of the unstable portions of phases 1 and 3. Figures 7*a* and 7*b* are similar to

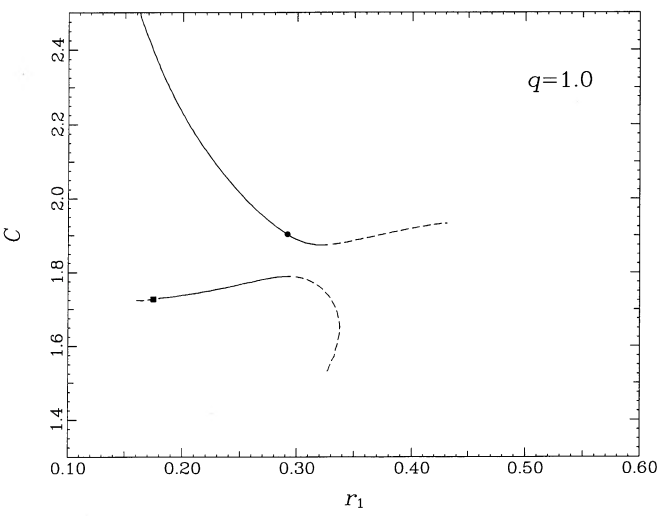

FIG. 6*a*

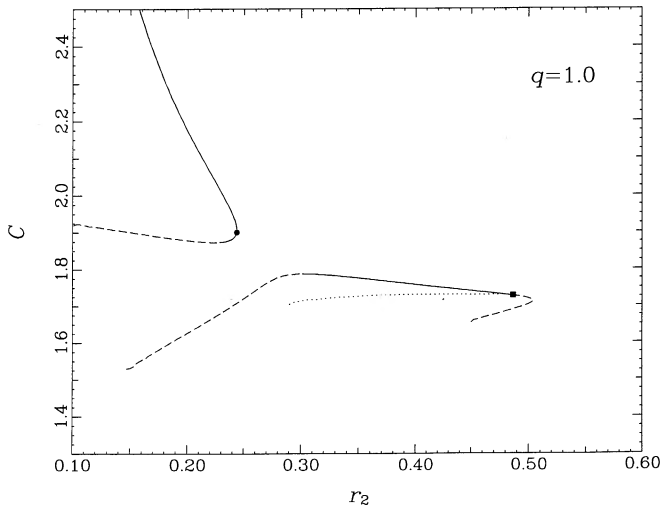

FIG. 6*b*

FIG. 6.—Periodic orbits for a binary system with mass ratio 1.0. Singly periodic orbits in the corotating frame are marked with solid lines if stable or with long-dashed lines if not. Doubly periodic orbits are marked with a short-dashed line.

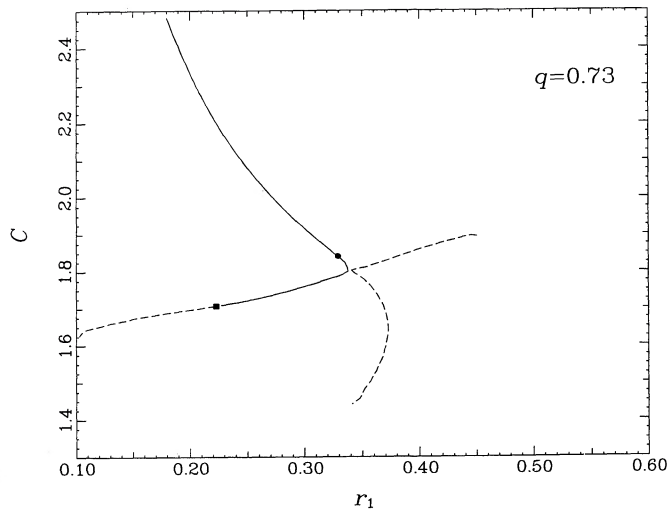

FIG. 7a

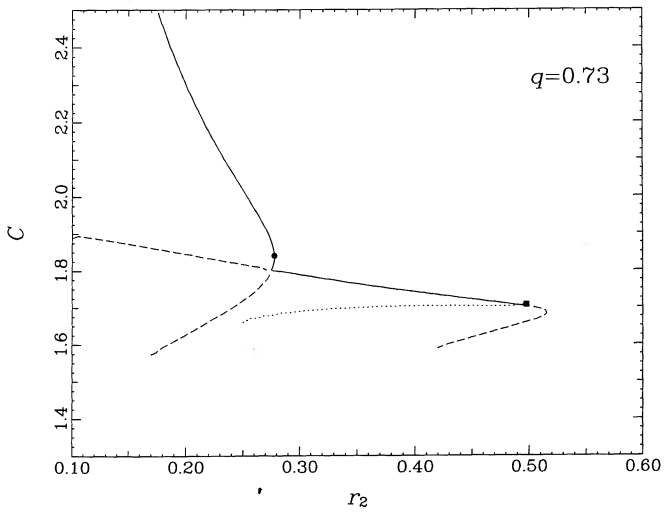

FIG. 7b

FIG. 7.—Periodic orbits for a binary system with mass ratio 0.73

Figures 6*a* and 6*b*, but for the $q = 0.73$ case to illustrate the orbits after this connection. The last nonintersecting point is still an inflection on the r_2 side, but after the reconnection this inflection is a small deviation. The lone stability transition occurs at the intersection with the class II orbit family.

A3. $q_2 = 0.730$

At q_2 the inflection on the r_2 side that had determined the last nonintersecting orbit has straightened out. The last nonintersecting orbit, therefore, is suddenly at a larger radius determined by the double-valued r_1 curve. Paczyński (1977) notes this bifurcation in his Figure 2 at this point but does not investigate the region in detail.

A4. $q_3 = 0.33$

At q_3 a new region of instability begins, marked by the appearance of two new families of doubly periodic orbits, both class II. Also at this point, the former class II family suddenly becomes a class I. This is the first appearance of the unstable region of the Whitehurst model. Figures 8*a* and 8*b* are similar to Figures 6*a* and 6*b*, but for the $q = 0.32$ case to illustrate behavior just beyond q_3. We mark the intersections of all three doubly periodic orbits with the singly periodic family, noting the change to instability, back briefly to stability, and again to instability. The new region of instability lies outside the last nonintersecting orbit.

A5. $q_4 = 0.31$

At q_4 the outer class II family crosses the class I family. Nonetheless, both above and below q_4 each intersection with the singly periodic orbits indicates a transition in stability.

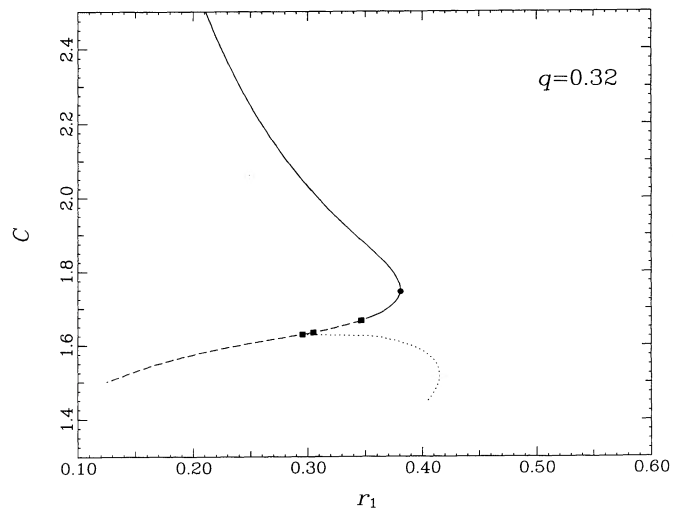

FIG. 8a

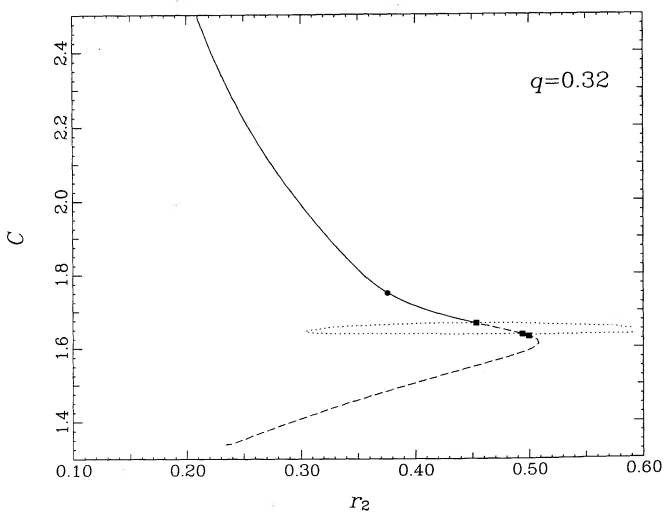

FIG. 8b

FIG. 8.—Periodic orbits for a binary system with mass ratio 0.32

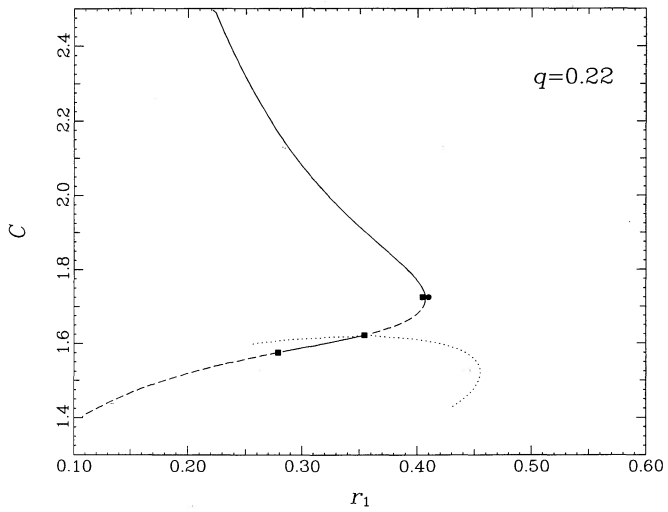

FIG. 9a

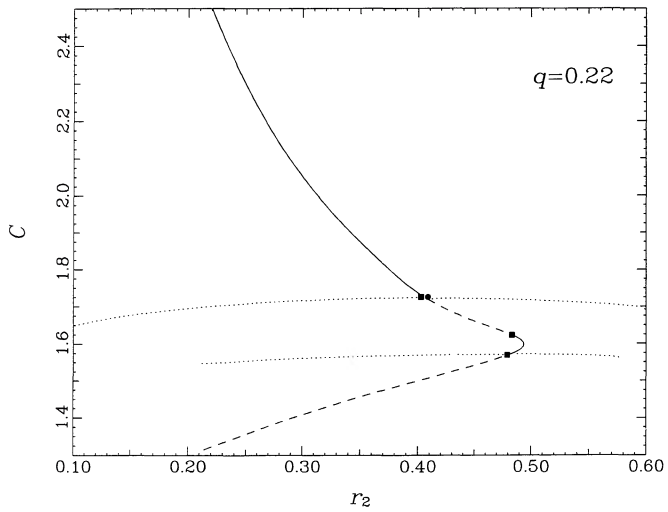

FIG. 9b

FIG. 9.—Periodic orbits for a binary system with mass ratio 0.22

A6. $q_5 = 0.22$

At q_5 the intersection with the first class II family now coincides with the last nonintersecting orbit. Figures 9*a* and 9*b* are similar to Figures 6*a* and 6*b*, but for the $q = q_5$ case. For smaller values of q the outer portion of an accretion disk truncated near the last nonintersecting orbit will be unstable. Hence q_5 is the important critical point for the Whitehurst (1988) model.

A7. $q_6 = 0.16$

At q_6 the lower class II orbit, which had been moving to steadily lower C values, ceases to intersect the singly periodic orbit family. This corresponds to the abrupt termination of the class II line in Figure 4.

A8. $q_7 = 0.16$

At q_7 the peak magnitude of the instability parameter between the upper class II orbit and the class I orbit reaches a maximum of 1.28 as shown in Figure 5.

A9. $q_8 = 0.08$

At q_8 the class I family intersects the singly periodic orbit family at the last nonintersecting point. For smaller values of q only an annulus of an accretion disk truncated near the last nonintersecting orbit will be unstable. As q goes to zero, this annulus does not disappear but becomes an ever narrower band around particle orbits at 3 times the orbital frequency. The maximum value of the instability parameter also decreases, going asymptotically to unity.

REFERENCES

Augusteijn, T., & Della Valle, M. 1990, IAU Circ., No. 5048
Bailey, J. 1990, MNRAS, 243, 57
Bond, H. E., Kemper, E., & Mattei, J. A. 1982, ApJ, 260, L79
Chen, J.-S., Lie, X.-W., & Wei, M.-Z. 1991, A&A, 242, 397
Cook, W. C., & Warner, B. 1984, MNRAS, 207, 705
Feinswog, L., Szkody, P., & Garnavich, P. 1988, AJ, 96, 1702
Gilliland, R. L. 1982a, ApJ, 254, 653
———. 1982b, ApJ, 258, 576
Gilliland, R. L., Kemper, E., & Suntzeff, N. 1986, ApJ, 301, 252
Grindlay, J. E., Bailyn, C. D., Cohn, H., Lugger, P. M., Thorstensen, J. R., & Wegner, G. 1988, ApJ, 334, L25
Hempelmann, A., & Kurths, J. 1990, A&A, 232, 356
Hirose, M., & Osaki, Y. 1990, PASJ, 42, 135
Horne, K., Wood, J. H., & Steining, R. F. 1991, ApJ, 378, 271
Howell, S. B., & Szkody, P. 1988, PASP, 100, 224
Kato, T., & Fujino, S. 1991, Var. Star Bull. Japan, 3, 10
Kuulkers, E. 1990, Master's thesis, Univ. Amsterdam
Naylor, T., Bath, G. T., Charles, P. A., Hassall, B. J. M., Berriman, G., Warner, B., Bailey, J., & Reinsch, K. 1987, MNRAS, 229, 183
O'Donoghue, D. 1987, Ap&SS, 136, 247
———. 1990, MNRAS, 246, 29
O'Donoghue, D., Chen, J., Marang, F., Mittaz, J. P. D., Winkler, H., & Warner, B. 1991, MNRAS, 250, 363
Osaki, Y. 1985, A&A, 144, 369
———. 1989, PASJ, 41, 1005
Paczyński, B. 1977, ApJ, 216, 822
Papaloizou, J., & Pringle, J. E. 1979, MNRAS, 189, 293
Patterson, J. 1979, AJ, 84, 804
———. 1984, ApJS, 54, 443
Patterson, J., McGraw, J. T., Colman, L., & Africano, J. L. 1981, ApJ, 248, 1067
Piotrowski, S. L., & Ziolkowski, K. 1970, Ap&SS, 8, 66
Rappaport, S., & Joss, P. C. 1984, ApJ, 283, 232
Richter, G. A. 1992, Proc. Viña del Mar Workshop on Cataclysmic Variable Stars, ed. N. Vogt (San Francisco: ASP), in press
Ritter, H. 1990, A&AS, 85, 1179
Robinson, E. L., Nather, R. E., & Patterson, J. 1978, ApJ, 219, 168
Robinson, E. L., Shafter, A. W., Hill, J. A., Wood, M. A., & Mattei, J. A. 1987, ApJ, 313, 772
Schoembs, R. 1986, A&A, 158, 233
Schoembs, R., & Vogt, N. 1981, A&A, 97, 185
Semeniuk, I. 1980, A&AS, 39, 29
Shafter, A. W., & Hessman, F. V. 1987, AJ, 95, 178
Shafter, A. W., & Szkody, P. 1984, ApJ, 276, 305
Shafter, A. W., Szkody, P., & Thorstensen, J. R. 1986, ApJ, 308, 765
Smak, J. 1984, Acta Astron., 34, 161
Stolz, B., & Schoembs, R. 1984, A&A, 132, 187
Szebehely, V. 1967, Theory of Orbits: The Restricted Problem of Three Bodies (New York: Academic)
Szkody, P., & Feinswog, L. 1988, ApJ, 334, 422
Szkody, P., Howell, S. B., Mateo, M., & Kreidl, T. J. 1989, PASP, 101, 899
Szkody, P., Shafter, A. W., & Cowley, A. P. 1984, ApJ, 282, 236
Thorstensen, J. R., Wade, R. A., & Oke, J. B. 1986, ApJ, 309, 721

Tuohy, I. R., Remillard, R. A., Brissenden, R. J. V., & Bradt, H. V. 1990, ApJ, 359, 204
Udalski, A. 1989, IAU Circ., No. 4774
Udalski, A., & Mattei, J. A. 1989, IAU Circ., No. 4885
Udalski, A., & Szymanski, M. 1988, Acta Astron., 38, 215
van der Woerd, H., & van Paradijs, J. 1987, MNRAS, 224, 271
van Paradijs, J., van der Klis, M., & Pedersen, H. 1989, A&A, 225, L5
Vogt, N. 1974, A&A, 36, 369
———. 1980, A&A, 88, 66
———. 1982, ApJ, 252, 653
———. 1983, A&A, 118, 95
Vogt, N., & Semeniuk, I. 1980, A&A, 89, 223
Warner, B. 1985, Proc. NATO Advanced Study Institute on Interacting Binaries, ed. P. P. Eggleton & J. E. Pringle (Dordrecht: Reidel), 367
Warner, B., & Livio, M. 1987, ApJ, 322, L95
Warner, B., O'Donoghue, D., & Wargau, W. 1989, MNRAS, 238, 73
Whitehurst, R. 1988, MNRAS, 232, 35
Whitehurst, R., Bath, G. T., & Charles, P. A. 1984, Nature, 309, 768
Whitehurst, R., & King, A. 1991, MNRAS, 249, 25
Wood, J., Horne, K., Berriman, G., & Wade, R. A. 1989, ApJ, 341, 974
Wood, J., Horne, K., Berriman, G., Wade, R. A., O'Donoghue, D., Warner, B. 1986, MNRAS, 219, 629
Zhang, E. H., Robinson, E. L., & Nather, R. E. 1986, ApJ, 305, 740